ACS Macro Letters

Open Access

pubs.acs.org/macroletters

Letter

Ellipsometric Characterization of Network Topology Transition in Vitrimers

Yuming Wang, Jaylen Davis, Travis L. Thornell, Sergei Nazarenko, Derek L. Patton, Yoan C. Simon,* and Zhe Qiang*

Cite This: *ACS Macro Lett.* 2025, 14, 1801−1807

Read Online

ABSTRACT: Vitrimers are an emerging class of covalent adaptable networks, which can be reprocessed at elevated temperatures while preserving crosslinking density. In these systems, the onset temperature of bond exchange is often dubbed "topology freezing transition temperature (T_v)" and is characterized by a sharp reduction in material viscosity. Here, we provide a universal and external stress-free method to determine T_v in submicrometer (<μm) supported films, by measuring their thickness change as a function of temperature by ellipsometry. This study investigated a range of vitrimer systems, including catalyst-free, externally catalyzed, and internally catalyzed networks, to confirm the general applicability of our approach. We demonstrate the high sensitivity of ellipsometry in detecting changes in the apparent thermal expansion behaviors of vitrimer films, specifically linked to the onset of bond exchange in vitrimers, which is distinguished from most other methods that primarily capture macroscopic thermomechanical behaviors. Our results also suggest that the mechanism by which ellipsometry reveals the T_v in vitrimers is governed by their change in relaxation dynamics, which are fundamentally distinct from the thermodynamically driven glass transition observed in conventional polymers. We believe the ellipsometric method can not only streamline the characterization of T_v in vitrimers but also provide deeper insights into their dynamic exchange mechanisms by distinguishing between their microscopic and macroscopic properties.

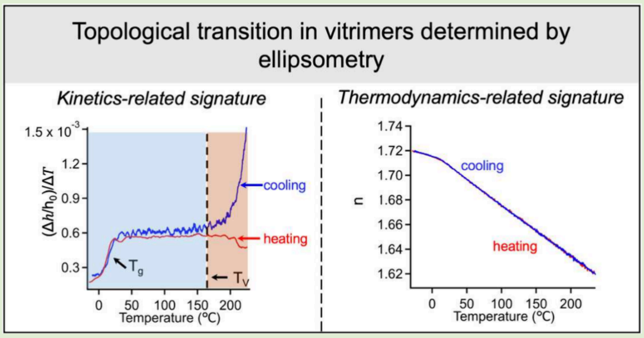

Vitrimers have garnered significant attention in the polymer community over the past decade due to their unique capability to exhibit reduced viscosity at elevated temperatures while maintaining a covalent network structure.[1−6] In these polymers, the topological rearrangement of the network typically can occur at a characteristic temperature, often referred to as the topology freezing transition temperature (T_v).[7] Specifically, when the material is below T_v, it behaves similarly to traditional crosslinked materials.[1,8,9] Upon heating above both T_v and T_g (glass transition temperature), the network becomes dynamic and reversible, allowing for flow and reprocessing. This unique ability of vitrimers makes them particularly promising for many advanced applications such as self-healing materials[10−12] and reprocessable thermosets,[13−15] providing potential to tackle challenges in material circularity. Notably, characterization of T_v is crucial for the rational implementation of vitrimer materials. Conventional methods for understanding T_v, such as stress relaxation,[15−19] creep measurements,[20−22] and rheology[18,23−26] typically focus on determining macroscopic material kinetics with the presence of external forces.[27] While these techniques provide valuable insights into the temperature- and/or strain-dependent thermomechanical responsess of vitrimers, external forces applied during measurements could impact polymer relaxation behaviors and possibly the activation energy required for dynamic bond exchange occurring,[28] potentially leading to discrepancies in the observed T_v across different conditions.[21] Several recent efforts have demonstrated external stress-free measurement approaches to characterize T_v, such as using aggregation-induced emission (AIE) dyes to detect sample free volume,[29] small-angle X-ray scattering (SAXS) to probe mesoscale structural rearrangements,[30,31] and temperature-modulated optical refractometry to quantify changes in refractive index as materials surpass T_v.[32] However, these methods seem to lead to differing conclusions regarding the mechanisms underlying T_v and their influence on the thermodynamic and kinetic properties of vitrimers, leaving important questions open for the field to address.

Furthermore, most methods for determining T_v have to date been limited to bulk material samples, making them less

Received: September 22, 2025
Revised: November 4, 2025
Accepted: November 7, 2025
Published: November 14, 2025

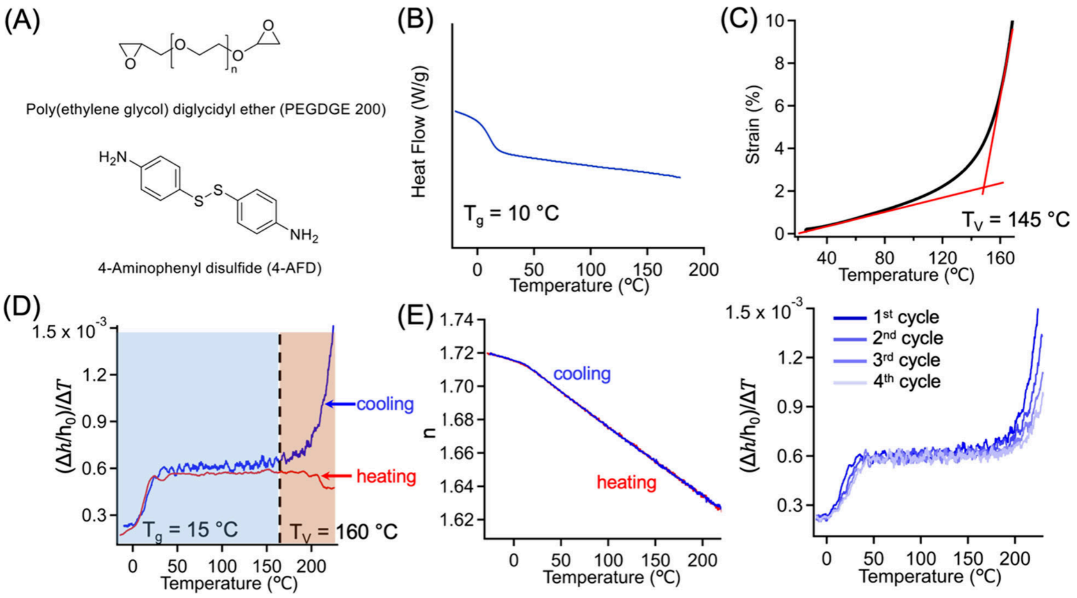

Figure 1. (A) Chemical structure of PEGDGE and 4-aminophenyl disulfide for preparing catalyst-free vitrimers. (B) DSC results (obtained from the 2nd heating cycle) for bulk vitrimer samples. (C) Non-isothermal creep measurement for disulfide-based vitrimer with an applied stress of 5 kPa. (D) Plot of $\frac{\Delta h / h_0}{\Delta T}$ vs temperature for disulfide-based vitrimer films obtained during cooling (blue) and heating (red) cycles. The change from light blue region to orange region represents the transition at T_v. (E) Refractive index (n) as a function of temperature for disulfide-based vitrimer films derived obtained during cooling (blue) and heating (red) cycle. (F) Plot of $\frac{\Delta h / h_0}{\Delta T}$ vs temperature for disulfide-based vitrimer films as a function of cycle number. The vitrimer film thickness was approximately 200 nm.

suitable for studying vitrimer thin films, which are becoming increasingly important in applications such as flexible electronics,[33−35] coatings,[36−38] and biomedical devices.[39−41] There is therefore a strong need to develop alternative methods to directly access the change in network topology rearrangement of vitrimer films. Ellipsometry is a well-established method to study thermal transitions in polymer thin films.[42−46] For instance, using this method, the T_g of polymer films can be determined by quantifying the change in thickness or thermal expansion coefficients between the rubbery and glassy states.[47−49] We propose to use ellipsometry to directly determine the T_v of vitrimers by characterizing film thickness as a function of temperature. This study focuses on understanding vitrimer systems in which T_v is higher than T_g. We established that, above T_v, bond exchange of crosslinkers mediates network relaxation and reduces viscosity, which in turn significantly alter the internal surface tension, leading to a distinct thermal expansion response in vitrimer thin films. This behavior is consistent across all vitrimer systems studied and is absent in permanently crosslinked networks. Our method eliminates the need of using external forces or guest molecules for enabling direct characterization of T_v in thin films with minimal material consumption.

This study first focused on an aromatic disulfide vitrimer as a model system, prepared by crosslinking poly(ethylene glycol) diglycidyl ether (PEGDGE, molecular weight is 200 g/mol) with 4,4′-aminophenyl disulfide (4-AFD) via epoxide−amine ring-opening polymerization (Figure 1(A)). In this network, embedded S−S linkages provide dynamic covalent crosslinks that undergo thermally activated disulfide exchange above T_v with the absence of a catalyst,[50] allowing topology rearrangement while preserving crosslink density. Bulk samples exhibit a T_g of approximately 10 °C, as determined by differential scanning calorimetry (DSC, Figure 1(B)). Reaction completion in thin films was verified by FTIR (disappearance of the aliphatic epoxide ring band near ∼910 cm^{-1} and increase of −OH signal near ∼3350 cm^{-1}, Figure S1) and gel-fraction measurements; an insoluble content of ∼70% was achieved after 1 h of curing at 150 °C (Figure S2). Figure 1(C) presents the non-isothermal creep results for bulk samples under an applied stress of 5 kPa, from which the T_v of bulk samples was determined to be at approximately 145 °C. Note that in some previous studies, T_v was defined as the temperature at which the strain begins to deviate from the linear trend at the end rubbery plateau range.[1,21] Here, we chose to determine T_v as the intersection point of linear fits applied to distinct temperature regimes.[16]

We aimed to demonstrate that ellipsometry method can be used to characterize T_v in thin films of vitrimers without the need for external forces, simply by analyzing the changes in $\frac{\Delta h / h_0}{\Delta T}$ as a function of temperature using eq 1 below,

$$\frac{\Delta h/h_0}{\Delta T} = \frac{h\left(T + \frac{\Delta T}{2}\right) - h\left(T - \frac{\Delta T}{2}\right)}{h_0 \Delta T} \tag{1}$$

where $\frac{\Delta h / h_0}{\Delta T}$ is the temperature-dependent normalized apparent thermal expansivity of polymer thin films, h is the temperature-dependent thickness, h_0 is the initial polymer film thickness, and ΔT is the differentiation range, which was set to be 5 °C. Ellipsometry is a well-established method to detect thermal transitions in polymer thin films, including widely used for T_g characterization, which can provide reliable data with minimal sample consumption. As shown in Figure 1(D), we observed two distinct changes in the plot of $\frac{\Delta h / h_0}{\Delta T}$ versus temperature, corresponding to the T_g and T_v at 15 and 160 °C, respectively. The polymer thin film T_g is comparable with DSC results, indicating that a film thickness of approximately 200

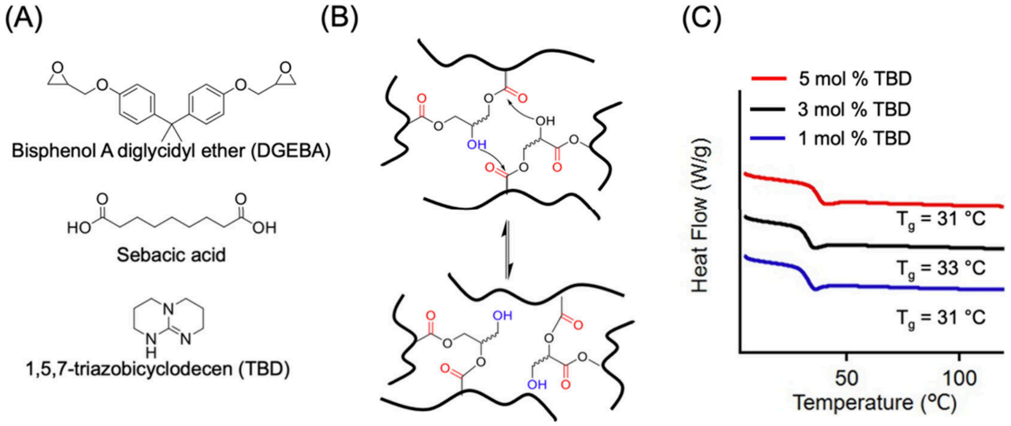

Figure 2. (A) Chemical structure of DGEBA, sebacic acid, and TBD (serving as a catalyst). (B) A simplified illustration of the topological bond exchange via transesterification mechanism. (C) DSC results (obtained from the 2nd heating cycle) for bulk vitrimer samples containing 1, 3, and 5 mol % TBD, respectively.

nm does not lead to confinement effects that significantly alter polymer segmental dynamics. Notably, the apparent thermal expansion response is reversible and consistent across heating and cooling near T_g, but it differs markedly in the vicinity of T_v. Upon heating above T_v, $\frac{\Delta h / h_0}{\Delta T}$ decreases because thermally activated bond exchange drives internal-surface-tension–mediated contraction/shrinkage (unidirectional and out-of-plane) that opposes thermal expansion, lowering the apparent expansion coefficient. During cooling to below T_v, $\frac{\Delta h / h_0}{\Delta T}$ drops more substantially, as intrinsic thermal contraction and the bond exchange-induced vitrimer shrinkage established above T_v act in concert. This competition on heating and cooperation on cooling leads to the observed difference around T_v, while dimensional shrinkage upon surpassing T_v is a well-documented phenomenon in vitrimer systems,[27,32] and our thermomechanical analysis (TMA) results similarly show a sharp reduction in bulk sample dimensions above T_v (Figure S3).

These results of vitrimer films shown in Figure 1D are intriguing and suggest that the mechanism probed by ellipsometry for characterizing T_v may be fundamentally distinct from that underlying T_g. It is important to emphasize that efforts to fully understand the topological transition of vitrimers and its impact on their free volume and apparent thermal expansion behavior are still ongoing. Particularly, molecular dynamics simulations with reactive force fields performed by Perego et al.,[51] found that exceeding T_v in vitrimers leads to a higher thermal expansion coefficient (α(T)) compared to permanently cross-linked systems. This increase was attributed to bond exchange processes generating additional free volume and thus a larger specific volume. By contrast, permanently crosslinked systems exhibited only minimal changes in α(T) with increasing temperature. These simulation findings are consistent with some experimental studies, such as using AIE fluorophores to assess local free volume within samples above T_v.[29] However, other reports potentially challenged this interpretation. For example, scattering methods have been used to probe vitrimer structure across different length scales. It was found that polymer chains exhibited the same apparent thermal expansion coefficient across the entire viscoelastic region, while the network structural transition surpassing T_v emerges only at the mesoscale.[30]

To further understand the mechanistic origin of T_v effects on vitrimer films, we determined their refractive index as a function of temperature from ellipsometry (Figure 1(E)). When the temperature is higher than T_g, it increased linearly with temperature and showed no anomaly upon crossing T_v, indicating very limited free volume change within our measurement window. This result supports the interpretation that the apparent changes in thermal expansion behavior of vitrimer films arise primarily from relaxation kinetics (i.e., reduced viscosity) and bond exchange-mediated internal surface tension, rather than from thermodynamic free volume variations. It is possible that any transient free volume fluctuations were likely not resolved if bond-exchange kinetics are sufficiently fast to appear quasi-equilibrated at our temporal and spatial resolution. Notably, our observations seem to be similar to a recent report. Specifically, Andreas et al.[32] employed TMA and temperature-modulated optical refractometry (TMOR) to characterize the $\alpha(T)$ of vitrimers as a function of temperature. Their TMA results from cooling showed a clear increase in apparent thermal expansivity upon surpassing T_v, when materials transited from viscoelastic solid state to viscoelastic liquid state, agreeing well with our data shown in Figure 1(D). In contrast, TMOR measurements indicated a nearly constant $\alpha(T)$ across T_v for bulk samples, suggesting a minimal change in the sample free volume, which is consistent with our findings in Figure 1(E). Here, we were able to obtain both temperature-dependent thermal-expansion behavior and refractive index from the same measurement, supporting that relaxation kinetics—rather than thermodynamic changes—can provide the most sensitive signals for characterizing the T_v. Moreover, Figure 1(F) shows the changes in $\frac{\Delta h / h_0}{\Delta T}$ as a function of temperature over successive heating–cooling cycles. These thermal cycles do not alter the T_v observed in our system; however, when above T_v, the magnitude of temperature-dependent change in $\frac{\Delta h / h_0}{\Delta T}$ gradually decreases upon repeated cycling. From the refractive index–temperature plots (Figure S4), we observed complete reversibility of the vitrimer films after four consecutive heating–cooling cycles, as further supported by the unchanged T_g values shown in Figure 1(F). Therefore, the reduced apparent thermal expansion behavior in disulfide-based vitrimers can be attributed to irreversible sample deformation accumulated during repeated measurements.

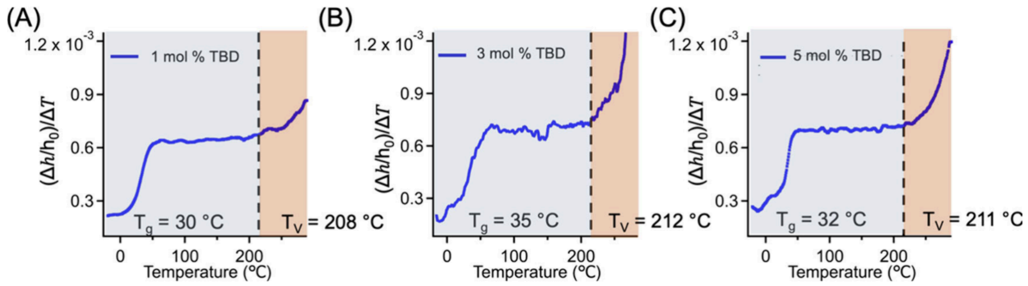

Figure 3. $\frac{\Delta h / h_0}{\Delta T}$ vs temperature plot of DGEBA-sebacic acid vitrimer systems with (A) 1 mol %, (B) 3 mol %, and (C) 5 mol % TBD. The change from blue to red represents the transition at T_v. All films have a thickness of approximately 150 nm.

We then investigated an established catalytic vitrimer systems using DGEBA and sebacic acid (Figure 2(A) and (B)) with TBD as a catalyst,[20] of which T_v has been extensively measured by various research groups using different techniques,[16,20,21,27] making it a suitable benchmark system. Specifically, TBD can promote transesterification at elevated temperatures via a dual-hydrogen bond activation, in which one nitrogen coordinates to the proton of the alcohol and the proton of the secondary amine coordinates to the oxygen of the carbonyl groups.[52−54] To determine the optimal curing conditions for the DGEBA-sebacic acid network, we performed DSC on the uncured bulk monomer mixture containing 5 mol % TBD. The exothermic peak in the corresponding thermogram (Figure S5(A), red) was around 170−180 °C.[20,21,27] The DSC thermogram of the cured samples show the complete disappearance of the exothermic peak (Figure S5(A)), indicating a completed reaction. FTIR (Figure S5(B)) further validated the effectiveness of the selected cure conditions through the appearance of stretching bands at 3500 and 1740 cm^{-1}, respectively, corresponding to the newly formed hydroxy groups and the carbonyl of ester groups after cross-linking. Concomitantly, the band around 1700 cm^{-1} corresponding to C═O stretching disappeared. Together, these results suggest successful esterification between carboxylic acid and epoxy groups in our model systems. When applied to thin films, curing for 15 min yielded a plateau in the insoluble content, reaching approximately 85% (based on film thickness, Figure S6). To confirm completed network formation under these conditions, we further examined the T_g as a function of curing time and found that films cured for 15 min at 180 °C exhibited an identical T_g to those cured for 2 h. This result indicates that a 15 min curing duration was sufficient and therefore adopted as the optimal condition for preparing DGEBA−sebacic acid vitrimer thin films. DSC thermograms of the bulk vitrimer samples (Figure 2(C)) at all catalyst loadings (1 to 5 mol %) showed a constant T_g around 31−33 °C, indicating that TBD does not act as a plasticizer to influence polymer segmental mobility.

Figure S8 presents the non-isothermal creep results for bulk samples of the DGEBA-sebacic acid vitrimers under 15 kPa. As the TBD loading increased from 1 mol % to 5 mol %, the T_v observed from nonisothermal creep in these vitrimer systems decreased from 247 to 207 °C, consistent with literature precedents quantitatively.[16] We note that the change in T_v with varying TBD amounts is often attributed to altered vitrimer creep relaxation kinetics and flow behaviors, as captured by thermomechanical measurements.[8] Increasing catalyst loading can result in faster and/or more frequent bond exchange at the crosslinks, reducing the characteristic relaxation time of the corresponding networks. Furthermore, Li et al. demonstrated that dynamic bonds may be sensitive to the magnitude of the applied force during measurements, with a larger force being able to further reduce the T_v characterized by material flow behaviors.[15] In our system, we also observed that changes in external forces impacted the T_v determined by non-isothermal creep (Figure S9). When the stress was increased from 10 to 50 kPa, the T_v of the 5 mol % TBD-loaded sample decreased significantly from 220 to 179 °C; our TMA result revealed a T_v of 205 °C for this sample, suggesting the T_v value could slightly vary depending on the characterization technique used (Figure S10). Similarly, Kaiser and co-workers examined the impact of external forces on the T_v of epoxy vitrimers with various acids and catalysts. They observed that T_v,[21] measured by non-isothermal creep, consistently decreased with increasing applied stress in all vitrimer systems, reaching a plateau at high stress levels.

While previous studies have shown that increasing catalyst loading may reduce the T_v of vitrimer networks, which was observed in our bulk samples via non-isothermal creep measurements (Figure S8), our ellipsometry data (Figure 3) indicates no noticeable change in the T_v of vitrimers (between 208 and 211 °C) with increased catalyst loading from 1 to 5 mol %. We believe this can be because conventional thermomechanical-based measurements characterize topological transitions in vitrimers by evaluating material flow activation energies and viscoelastic behaviors, which are often collectively governed by bond exchange dynamics, segmental mobility, crosslinking density, and network heterogeneity. Our ellipsometry measurements could more directly capture intrinsic material responses (e.g., the onset temperature for bond exchange), under which the influence of catalyst loading becomes significantly less pronounced. These results also indicate when above T_v, films with 1 mol % TBD possess a lower apparent thermal expansion coefficient, in contrast to the comparable values observed for 3 mol % and 5 mol % TBD. This trend implies that the bond-exchange-mediated relaxation kinetics in vitrimer thin films are enhanced once the catalyst loading surpasses roughly 3 mol %. We note that Yang and co-workers reported a similar observation to ours: using AIE fluorophore as a guest molecule to probe free volume changes, they found unchanged T_v values were found despite varying catalyst loading in transesterification-based vitrimer networks.[34] Interestingly, like here, their approach does not require external forces. Collectively, these findings can explain why T_v values remained consistent in our measurements, despite different catalyst loading content. Moreover, we prepared a model permanently cross-linked polymer film from 4,4’-methylenedianiline and 1,4-butanediol diglycidyl

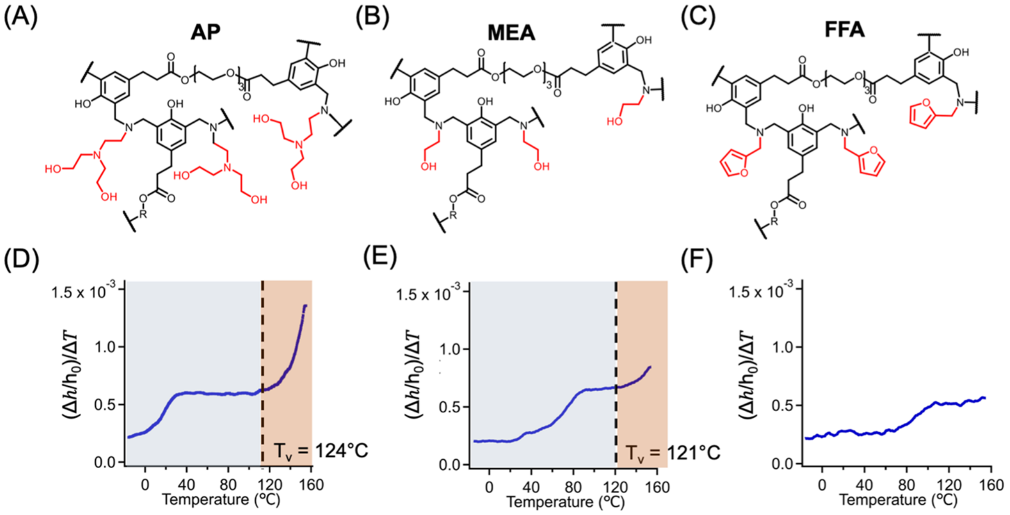

Figure 4. Chemical structure of different cross-linked networks, including vitrimers prepared from (A) aminopropyl diethylamine (AP), (B) monoethanolamine (MEA) precursors, and (C) permanently crosslinked network prepared from furfurylamine (FFA) precursor, and their corresponding $\frac{\Delta h / h_0}{\Delta T}$ vs temperature plot for (D) AP, (E) MEA, and (F) FFA thin films, respectively. The change from blue to red represents the transition at T_v. Film thickness of all samples is approximately 150 nm.

ether in a 1:2 molar ratio (Figures S11). The film exhibits a T_g around 50 °C (Figure S12) similar to T_g characterized by DSC measurements (Figure S11(B)). No distinct change in $\frac{\Delta h / h_0}{\Delta T}$ was observed at temperatures above T_g, and only a minimal increase was detected, which aligns with previously reported simulation results.[51]

We further studied the effect of cooling rate on the apparent T_v measured by ellipsometry, using 5 mol % TBD-loaded vitrimer films as a model system. As shown in Figure S13, changing the cooling rate from 10 to 2 °C/min does not have a noticable impact on T_v, slightly increasing from 209 to 211 °C. Moreover, multiple heat−cool cycles (from −30 to 300 °C) were performed on the same sample to assess how thermal history affects both T_g and T_v. Here, a 5 mol % TBD-loaded film was subjected to a total of 3 heating and cooling cycles at a rate of 5 °C/min. During the third cycle (Figure S14), T_g remained largely unchanged, while the T_v transition became less pronounced. Because this effect was more pronounced than in the disulfide vitrimer model system, we attribute it to the thermal degradation and loss of TBD catalytic activity during repeated heating, as previously reported.[55] Moreover, we investigated the impact of film casting method on T_v measurements. Specifically, vitrimer films (~150 nm) were prepared using a dip casting method, employing the same solution used for spin-casting. Ellipsometry curves indicated that both T_g (around 30 °C) and T_v (around 210 °C) were similar regardless of whether the film was spin-coated on the substrate or dip-coated (Figure S15).

To further demonstrate the versatility of this method, we studied additional benzoxazine-based vitrimers (Figure 4(A−C)), where dynamic bond exchange in the cross-linking units is self-catalyzed (Figure S16). Aminopropyl diethylamine (AP) and monoethanolamine (MEA) were used as precursors for vitrimer samples, while furfurylamine (FFA) was served as the precursor for preparing permanently cross-linked thermoset system. As presented in Figure S17 and Figure 4(D−F), ellipsometry measurements demonstrate a distinct T_v transition in the $\frac{\Delta h / h_0}{\Delta T}$−temperature plots for both vitrimer systems, with T_v observed at approximately 124 °C for AP and 121 °C for MEA, respectively. These transitions correspond to the onset of dynamic bond exchange in the systems. In contrast, the FFA thermoset exhibits a linear relationship between thickness and temperature, consistent with its rubbery state behavior and indicates the absence of dynamic bond exchange. Our ellipsometry data corroborates the nonisothermal creep results (Figure S18), with T_v values of 139 and 150 °C for AP and MEA respectively. This consistency confirms the reliability of ellipsometric measurement method in detecting the topology freezing transition, as the FFA results further confirm that our method effectively differentiates between dynamic vitrimer networks and permanently cross-linked thermosets.

In summary, this study introduced a simple and efficient ellipsometry-based method to measure the T_v of vitrimer thin films, offering potential for analyzing complex vitrimer systems. By comparing vitrimer films with permanently crosslinked thermoset systems, we observe a noticeable change in the thermal expansion behaviors of vitrimer films upon surpassing their T_v, as a result of their onset dynamic exchange. We attribute this shift primarily to kinetic factors in vitrimer samples above T_v, including bond-exchange-mediated changes induced internal surface tension and reduced viscosity. Notably, in our work, it is found that catalyst loading ratio and temperature ramping rate did not influence the T_v measured by ellipsometry, in contrast to conventional thermomechanical-based methods. This distinction could arise from the ability of ellipsometry to directly capture dynamic bond exchange at a microscopic scale without the interference of external forces. Although we understand that apparent T_v can be dependent on characterization methods and conditions, our method for determining T_v still offers distinct advantages including eliminating the use of guest molecules and external forces, which the latter can minimize sample deformation. Beyond improving our understanding of the dynamic exchange properties of vitrimers, this method can provide a critical tool for investigating confinement effects on vitrimer film behavior, paving the way for advancements in vitrimer applications in fields like coatings, electronics, and biomedical devices.

ASSOCIATED CONTENT

Supporting Information

The Supporting Information is available free of charge at https://pubs.acs.org/doi/10.1021/acsmacrolett.5c00640.

> Detailed experimental procedures, materials and methods; Comprehensive characterization of model vitrimer systems including DGEBA–sebacic acid/TBD (1–5 mol %) and disulfide-based PEGDGE/4-AFD networks; Insoluble content of thin films vs curing time; Ellipsometry data: thickness–temperature plots, refractive index–temperature data, and heating/cooling cycling studies; TMA and nonisothermal creep measurements for bulk samples; Additional analysis of permanently cross-linked network (PDF)

AUTHOR INFORMATION

Corresponding Authors

Yoan C. Simon – *School of Molecular Sciences, Arizona State University, Tempe, Arizona 85287, United States;* orcid.org/0000-0002-5235-6127; Email: yoan.simon@asu.edu

Zhe Qiang – *School of Polymer Science and Engineering, University of Southern Mississippi, Hattiesburg, Mississippi 39406, United States;* orcid.org/0000-0002-3539-9053; Email: zhe.qiang@usm.edu

Authors

Yuming Wang – *School of Polymer Science and Engineering, University of Southern Mississippi, Hattiesburg, Mississippi 39406, United States*

Jaylen Davis – *School of Polymer Science and Engineering, University of Southern Mississippi, Hattiesburg, Mississippi 39406, United States; Environmental Laboratory, U.S. Army Engineer Research and Development Center, Vicksburg, Mississippi 39180, United States*

Travis L. Thornell – *Geotechnical and Structures Laboratory, U.S. Army Engineer Research and Development Center, Vicksburg, Mississippi 39180, United States*

Sergei Nazarenko – *School of Polymer Science and Engineering, University of Southern Mississippi, Hattiesburg, Mississippi 39406, United States;* orcid.org/0000-0003-0538-5459

Derek L. Patton – *School of Polymer Science and Engineering, University of Southern Mississippi, Hattiesburg, Mississippi 39406, United States;* orcid.org/0000-0002-8738-4750

Complete contact information is available at: https://pubs.acs.org/10.1021/acsmacrolett.5c00640

Author Contributions

The manuscript was written through contributions of all authors.

Notes

The authors declare no competing financial interest.

ACKNOWLEDGMENTS

This work was partially supported by The U.S. Army Engineer Research and Development Center (ERDC) Contract #W912HZ21C0029, BAA 20-0110. Z.Q. acknowledged the support from the National Science Foundation (OIA-2316531). Y.C.S. also acknowledged for financial support by the National Science Foundation through the CAREER (1945092).

REFERENCES

(1) Montarnal, D.; Capelot, M.; Tournilhac, F.; Leibler, L. Silica-Like Malleable Materials from Permanent Organic Networks. *Science* **2011**, *334* (6058), 965–968.

(2) Zheng, J.; Png, Z. M.; Ng, S. H.; Tham, G. X.; Ye, E.; Goh, S. S.; Loh, X. J.; Li, Z. Vitrimers: Current research trends and their emerging applications. *Mater. Today* **2021**, *51*, 586–625.

(3) Schenk, V.; Labastie, K.; Destarac, M.; Olivier, P.; Guerre, M. Vitrimer composites: current status and future challenges. *Materials Advances* **2022**, *3* (22), 8012–8029.

(4) Guerre, M.; Taplan, C.; Winne, J. M.; Du Prez, F. E. Vitrimers: directing chemical reactivity to control material properties. *Chemical science* **2020**, *11* (19), 4855–4870.

(5) Adjaoud, A.; Trejo-Machin, A.; Puchot, L.; Verge, P. Polybenzoxazines: a sustainable platform for the design of fast responsive and catalyst-free vitrimers based on trans-esterification exchanges. *Polym. Chem.* **2021**, *12* (22), 3276–3289.

(6) Hubbard, A. M.; Ren, Y.; Sarvestani, A.; Konkolewicz, D.; Picu, C. R.; Roy, A. K.; Varshney, V.; Nepal, D. Recyclability of Vitrimer Materials: Impact of Catalyst and Processing Conditions. *ACS Omega* **2022**, *7* (33), 29125–29134.

(7) Legrand, A. l.; Soulié-Ziakovic, C. Silica-epoxy vitrimer nanocomposites. *Macromolecules* **2016**, *49* (16), 5893–5902.

(8) Capelot, M.; Unterlass, M. M.; Tournilhac, F.; Leibler, L. Catalytic Control of the Vitrimer Glass Transition. *ACS Macro Lett.* **2012**, *1* (7), 789–792.

(9) Capelot, M.; Montarnal, D.; Tournilhac, F.; Leibler, L. Metal-catalyzed transesterification for healing and assembling of thermosets. *Journal of the American chemical society* **2012**, *134* (18), 7664–7667.

(10) Yang, Y.; Xu, Y.; Ji, Y.; Wei, Y. Functional epoxy vitrimers and composites. *Prog. Mater. Sci.* **2021**, *120*, 100710.

(11) Yang, X.; Guo, L.; Xu, X.; Shang, S.; Liu, H. A fully bio-based epoxy vitrimer: Self-healing, triple-shape memory and reprocessing triggered by dynamic covalent bond exchange. *Materials & Design* **2020**, *186*, 108248.

(12) Xu, Y.; Dai, S.; Bi, L.; Jiang, J.; Zhang, H.; Chen, Y. Catalyst-free self-healing bio-based vitrimer for a recyclable, reprocessable, and self-adhered carbon fiber reinforced composite. *Chemical Engineering Journal* **2022**, *429*, 132518.

(13) Snyder, R. L.; Fortman, D. J.; De Hoe, G. X.; Hillmyer, M. A.; Dichtel, W. R. Reprocessable acid-degradable polycarbonate vitrimers. *Macromolecules* **2018**, *51* (2), 389–397.

(14) Fortman, D. J.; Brutman, J. P.; Cramer, C. J.; Hillmyer, M. A.; Dichtel, W. R. Mechanically activated, catalyst-free polyhydroxyurethane vitrimers. *J. Am. Chem. Soc.* **2015**, *137* (44), 14019–14022.

(15) Li, L.; Chen, X.; Jin, K.; Torkelson, J. M. Vitrimers designed both to strongly suppress creep and to recover original cross-link density after reprocessing: quantitative theory and experiments. *Macromolecules* **2018**, *51* (15), 5537–5546.

(16) Hubbard, A. M.; Ren, Y.; Konkolewicz, D.; Sarvestani, A.; Picu, C. R.; Kedziora, G. S.; Roy, A.; Varshney, V.; Nepal, D. Vitrimer transition temperature identification: coupling various thermomechanical methodologies. *ACS Applied Polymer Materials* **2021**, *3* (4), 1756–1766.

(17) Chen, M.; Zhou, L.; Wu, Y.; Zhao, X.; Zhang, Y. Rapid stress relaxation and moderate temperature of malleability enabled by the synergy of disulfide metathesis and carboxylate transesterification in epoxy vitrimers. *ACS Macro Lett.* **2019**, *8* (3), 255–260.

(18) Dugas, L. D.; Walker, W. D.; Shankar, R.; Hoppmeyer, K. S.; Thornell, T. L.; Morgan, S. E.; Storey, R. F.; Patton, D. L.; Simon, Y. C. Diketoenamine-Based Vitrimers via Thiol-ene Photopolymerization. *Macromol. Rapid Commun.* **2022**, *43* (24), 2200249.

(19) Soman, B.; Schweizer, K. S.; Evans, C. M. Fragile Glass Formation and Non-Arrhenius Upturns in Ethylene Vitrimers

Revealed by Dielectric Spectroscopy. *Macromolecules* **2023**, *56* (1), 166−176.

(20) Hubbard, A. M.; Ren, Y.; Picu, C. R.; Sarvestani, A.; Konkolewicz, D.; Roy, A. K.; Varshney, V.; Nepal, D. Creep mechanics of epoxy vitrimer materials. *ACS Applied Polymer Materials* **2022**, *4* (6), 4254−4263.

(21) Kaiser, S.; Novak, P.; Giebler, M.; Gschwandl, M.; Novak, P.; Pilz, G.; Morak, M.; Schlögl, S. The crucial role of external force in the estimation of the topology freezing transition temperature of vitrimers by elongational creep measurements. *Polymer* **2020**, *204*, 122804.

(22) Porath, L.; Huang, J.; Ramlawi, N.; Derkaloustian, M.; Ewoldt, R. H.; Evans, C. M. Relaxation of vitrimers with kinetically distinct mixed dynamic bonds. *Macromolecules* **2022**, *55* (11), 4450−4458.

(23) Fang, H.; Ye, W.; Ding, Y.; Winter, H. H. Rheology of the critical transition state of an epoxy vitrimer. *Macromolecules* **2020**, *53* (12), 4855−4862.

(24) Ricarte, R. G.; Tournilhac, F.; Cloître, M.; Leibler, L. Linear Viscoelasticity and Flow of Self-Assembled Vitrimers: The Case of a Polyethylene/Dioxaborolane System. *Macromolecules* **2020**, *53* (5), 1852−1866.

(25) Ricarte, R. G.; Shanbhag, S. A tutorial review of linear rheology for polymer chemists: basics and best practices for covalent adaptable networks. *Polym. Chem.* **2024**, *15* (9), 815−846.

(26) Soman, B.; Evans, C. M. Effect of precise linker length, bond density, and broad temperature window on the rheological properties of ethylene vitrimers. *Soft Matter* **2021**, *17* (13), 3569−3577.

(27) Hubbard, A. M.; Ren, Y.; Sarvestani, A.; Picu, C. R.; Varshney, V.; Nepal, D. Thermomechanical analysis (TMA) of vitrimers. *Polym. Test.* **2023**, *118*, 107877.

(28) Song, Z.; Shen, T.; Vernerey, F. J.; Cai, S. Force-dependent bond dissociation explains the rate-dependent fracture of vitrimers. *Soft Matter* **2021**, *17* (27), 6669−6674.

(29) Yang, Y.; Zhang, S.; Zhang, X.; Gao, L.; Wei, Y.; Ji, Y. Detecting topology freezing transition temperature of vitrimers by AIE luminogens. *Nat. Commun.* **2019**, *10* (1), 3165.

(30) Arbe, A.; Alegría, A.; Colmenero, J.; Bhaumik, S.; Ntetsikas, K.; Hadjichristidis, N. Microscopic evidence for the topological transition in model vitrimers. *ACS Macro Lett.* **2023**, *12* (11), 1595−1601.

(31) Hayashi, M.; Suzuki, M.; Kito, T. Understanding the Topology Freezing Temperature of Vitrimer-Like Materials through Complementary Structural and Rheological Analyses for Phase-Separated Network. *ACS Macro Lett.* **2025**, *14* (2), 182−187.

(32) Klingler, A.; Reisinger, D.; Schlögl, S.; Wetzel, B.; Breuer, U.; Krüger, J.-K. Vitrimer Transition Phenomena from the Perspective of Thermal Volume Expansion and Shape (In) stability. *Macromolecules* **2024**, *57* (9), 4246−4253.

(33) Zhang, J.; Lei, Z.; Luo, S.; Jin, Y.; Qiu, L.; Zhang, W. Malleable and recyclable conductive mwcnt-vitrimer composite for flexible electronics. *ACS Applied Nano Materials* **2020**, *3* (5), 4845−4850.

(34) Yang, Y.; Pei, Z.; Li, Z.; Wei, Y.; Ji, Y. Making and remaking dynamic 3D structures by shining light on flat liquid crystalline vitrimer films without a mold. *Journal of the American chemical society* **2016**, *138* (7), 2118−2121.

(35) Deng, J.; Kuang, X.; Liu, R.; Ding, W.; Wang, A. C.; Lai, Y. C.; Dong, K.; Wen, Z.; Wang, Y.; Wang, L.; et al. Vitrimer elastomer-based jigsaw puzzle-like healable triboelectric nanogenerator for self-powered wearable electronics. *Adv. Mater.* **2018**, *30* (14), 1705918.

(36) Jouyandeh, M.; Tikhani, F.; Hampp, N.; Yazdi, D. A.; Zarrintaj, P.; Ganjali, M. R.; Saeb, M. R. Highly curable self-healing vitrimer-like cellulose-modified halloysite nanotube/epoxy nanocomposite coatings. *Chemical Engineering Journal* **2020**, *396*, 125196.

(37) Ma, J.; Porath, L. E.; Haque, M. F.; Sett, S.; Rabbi, K. F.; Nam, S.; Miljkovic, N.; Evans, C. M. Ultra-thin self-healing vitrimer coatings for durable hydrophobicity. *Nat. Commun.* **2021**, *12* (1), 5210.

(38) Zhang, S.; Liu, T.; Hao, C.; Mikkelsen, A.; Zhao, B.; Zhang, J. Hempseed oil-based covalent adaptable epoxy-amine network and its potential use for room-temperature curable coatings. *ACS Sustainable Chem. Eng.* **2020**, *8* (39), 14964−14974.

(39) Joe, J.; Shin, J.; Choi, Y.-S.; Hwang, J. H.; Kim, S. H.; Han, J.; Park, B.; Lee, W.; Park, S.; Kim, Y. S.; Kim, D.-G. A 4D Printable Shape Memory Vitrimer with Repairability and Recyclability through Network Architecture Tailoring from Commercial Poly(ε-caprolactone). *Advanced Science* **2021**, *8* (24), 2103682.

(40) Kuang, X.; Mu, Q.; Roach, D. J.; Qi, H. J. Shape-programmable and healable materials and devices using thermo-and photo-responsive vitrimer. *Multifunctional Materials* **2020**, *3* (4), 045001.

(41) Li, X.; Wang, L.; Li, Y.; Xu, S. Reprocessable, Self-Healing, Thermadapt Shape Memory Polycaprolactone via Robust Ester-Ester Interchanges Toward Kirigami-Tailored 4D Medical Devices. *ACS Applied Polymer Materials* **2023**, *5* (2), 1585−1595.

(42) Pye, J. E.; Roth, C. B. Two simultaneous mechanisms causing glass transition temperature reductions in high molecular weight freestanding polymer films as measured by transmission ellipsometry. *Physical review letters* **2011**, *107* (23), 235701.

(43) Kim, S.; Hewlett, S.; Roth, C.; Torkelson, J. Confinement effects on glass transition temperature, transition breadth, and expansivity: Comparison of ellipsometry and fluorescence measurements on polystyrene films. *Eur. Phys. J. E* **2009**, *30*, 83−92.

(44) Dalnoki-Veress, K.; Forrest, J.; Murray, C.; Gigault, C.; Dutcher, J. Molecular weight dependence of reductions in the glass transition temperature of thin, freely standing polymer films. *Phys. Rev. E* **2001**, *63* (3), 031801.

(45) White, R. P.; Buculei, D.; Beale, A. M.; Goovaerts, I.; Keddie, J. L.; Lipson, J. E. Spectroscopic ellipsometry as a route to thermodynamic characterization. *Soft Matter* **2022**, *18* (35), 6660−6673.

(46) Hajduk, B.; Bednarski, H.; Trzebicka, B. Temperature-Dependent Spectroscopic Ellipsometry of Thin Polymer Films. *J. Phys. Chem. B* **2020**, *124* (16), 3229−3251.

(47) Zhang, L.; Elupula, R.; Grayson, S. M.; Torkelson, J. M. Major Impact of Cyclic Chain Topology on the Tg-Confinement Effect of Supported Thin Films of Polystyrene. *Macromolecules* **2016**, *49* (1), 257−268.

(48) Bittrich, E.; Windrich, F.; Martens, D.; Bittrich, L.; Häussler, L.; Eichhorn, K.-J. Determination of the glass transition temperature in thin polymeric films used for microelectronic packaging by temperature-dependent spectroscopic ellipsometry. *Polym. Test.* **2017**, *64*, 48−54.

(49) Beaucage, G.; Composto, R.; Stein, R. S. Ellipsometric study of the glass transition and thermal expansion coefficients of thin polymer films. *J. Polym. Sci., Part B: Polym. Phys.* **1993**, *31* (3), 319−326.

(50) Azcune, I.; Odriozola, I. Aromatic disulfide crosslinks in polymer systems: Self-healing, reprocessability, recyclability and more. *Eur. Polym. J.* **2016**, *84*, 147−160.

(51) Perego, A.; Lazarenko, D.; Cloitre, M.; Khabaz, F. Microscopic dynamics and viscoelasticity of vitrimers. *Macromolecules* **2022**, *55* (17), 7605−7613.

(52) Fritz-Langhals, E. Unique Superbase TBD (1,5,7-Triazabicyclo[4.4.0]dec-5-ene): From Catalytic Activity and One-Pot Synthesis to Broader Application in Industrial Chemistry. *Org. Process Res. Dev.* **2022**, *26* (11), 3015−3023.

(53) Kiesewetter, M. K.; Scholten, M. D.; Kirn, N.; Weber, R. L.; Hedrick, J. L.; Waymouth, R. M. Cyclic Guanidine Organic Catalysts: What Is Magic About Triazabicyclodecene? *Journal of Organic Chemistry* **2009**, *74* (24), 9490−9496.

(54) Kim, J. G.; Lee, G. S.; Lee, A. Triazabicyclodecene: A versatile catalyst for polymer synthesis. *J. Polym. Sci.* **2024**, *62* (1), 42−91.

(55) Kaiho, S.; Hmayed, A. A. R.; Delle Chiaie, K. R.; Worch, J. C.; Dove, A. P. Designing thermally stable organocatalysts for poly (ethylene terephthalate) synthesis: Toward a one-pot, closed-loop chemical recycling system for PET. *Macromolecules* **2022**, *55* (23), 10628−10639.